Sigma J Eng Nat Sci, Vol. 41, No. 2, pp. 302–321, April, 2023

Sigma Journal of Engineering and Natural Sciences
Web page info: https://sigma.yildiz.edu.tr
DOI: 10.14744/sigma.2023.00040

Research Article

Prediction of the natural frequencies of various beams using regression machine learning models

Oguzhan DAS[1,*]

[1]*National Defence University, Air NCO Higher Vocational School, Department of Aeronautics Science, Izmir, 35000, Türkiye*

ARTICLE INFO

Article history
Received: 18 August 2021
Revised: 09 November 2021
Accepted: 01 January 2022

Keywords:
Natural Frequency Prediction; Finite Element Analysis; Beams; Artificial Intelligence; Machine Learning; Regression

ABSTRACT

Machine learning models are widely used for decades in various engineering applications, such as structural health monitoring, optimization of the properties of engineering systems or structures. For instance, in structural engineering, researchers have investigated machine learning techniques for the prediction of the natural frequencies, damage detection, and design optimization of beams, frames, plates, and many other structures. Using machine learning is advantageous since machine learning can reduce the cost and time consumption to solve real-world problems. These techniques do not require powerful computers and software, unlike numerical analysis methods to solve such problems. To benefit such positive aspects of the machine learning techniques, the prediction of the first ten natural frequencies of aluminum and steel very thin, thin, and thick beam structures under fixed-free, fixed-simply supported, and simply supported boundary conditions by using Radial Basis Function Regressor, Random Forest Regressor, Multilayer Perceptrons Regressor, and Support Vector Machine Regressor with Pearson VII Universal Function Kernel (Puk) has been presented. The dataset required for the analysis is obtained via the Finite Element Analysis considering Euler-Bernoulli and Timoshenko Beam Theories. The performance of the machine learning models has been investigated and compared by examining (i) the thickness-length ratio, (ii) boundary conditions, and (iii) natural frequencies of the beam structures. Results indicate that the considered regression machine learning models are effective in predicting the natural frequencies of beam structures. Among all four regression machine learning models, Support Vector Machine Regressor with Puk and Random Forest models are robust and accurately predict the natural frequency values of the structures by an average accuracy of 98.78% and 98.88% regardless of the boundary conditions and thickness-length ratio of beam structures. On the other hand, Radial Basis Function Regressor and Multilayer Perceptron Regressors predict the first ten natural frequencies by 96.36% and 94.17%, respectively.

Cite this article as: Das O. Prediction of the natural frequencies of various beams using regression machine learning models. Sigma J Eng Nat Sci 2023;41(2):302–321.

***Corresponding author.**
*E-mail address: odas@msu.edu.tr; droguzhandas@gmail.com; oguzhan.das@deu.edu.tr

This paper was recommended for publication in revised form by Regional Editor Amin Shahsavar

INTRODUCTION

Engineers and researchers performed various studies to understand the mechanical properties of materials and structures by conducting theoretical and experimental analyses [1-10]. In some cases, such analyses become costly and time-consuming due to the complexity of the problem. Therefore, researchers employed machine learning techniques since they not only give accurate results but also solve the cost and time-consuming problems. Thanks to this positive aspect, they are used in many engineering fields [11-17]. In structural engineering, machine learning has been especially used in structural health monitoring, optimization, and prediction of the properties of a system or a structure. Among such properties, the evaluation of the natural frequencies of structures is vital, especially in the designing phase, to understand whether the excessive vibrations cause issues such as failure due to resonance. Similarly, detecting damages on these structures is also essential since it provides an understanding of whether the structure can continue to operate or not. Therefore, engineers perform analyses and optimizations to obtain the natural frequencies for determining both the natural frequencies and the condition of the structure. Sometimes these analyses are being costly and take a long time for some applications in which an extensive range of parameters are examined. Researchers have investigated alternative approaches to provide fast and robust models to perform such analyses. Following the advancements in computer science, artificial intelligence has become popular as a powerful tool to solve complex, time-consuming, and costly problems. Scientists have studied various techniques to understand whether they are suitable for specific tasks in structural engineering. Some studies that existed in the literature, including machine learning applications in structures, are presented as follows. Laory et al. [18] examined Multiple Linear Regression, Artificial Neural Networks, Regression Tree, Support Vector Regression with RBF kernel, and Random Forest models to predict the natural frequency of the Tamar Suspension Bridge using 3-year continuous monitoring data. Besides, they investigated the effects of traffic loading and environmental factors on the natural frequencies. They concluded that Random Forest and Support Vector Regression with RBF kernels are the best models for such a problem. Avcar and Saplıoğlu [19] employed Artificial Neural Networks to estimate the first ten natural frequencies of beams, whose thickness-length ratio varies between 1/35-1/20. They investigated the effect of the transfer functions on the prediction performance considering various cases. They concluded that the effectiveness of the transfer functions depends on the experimental settings of the prediction. Dey et al. [20] used Artificial Neural Network (ANN) for uncertainty quantification in natural frequencies of composite plates. They trained the ANN model employing the Latin hypercube sample and quantified the stochastic first two natural frequencies via the trained ANN model. Banerjee et al. [21] used Cascade Forward Back Propagation Artificial Neural Network (CFBP) and Adaptive Fuzzy Inference Systems (ANFIS) to predict the first three natural frequencies of cracked beams. They employed Timoshenko Beam Theory to model the cracked structures. They found out that while ANFIS is better for the prediction of the first two natural frequencies, CFBP predicts the third natural frequency more accurately. Nikoo et al. [22] employed a Genetic Algorithm, Particle Swarm Optimization Algorithm, and Imperialist Competitive Algorithm to train an Artificial Neural Network to predict the first natural frequency of cantilever beam structures. They used a dataset with 100 samples for this purpose. They concluded that the Artificial Neural Network trained with Genetic Algorithm gives better prediction results when compared with other heuristic optimization techniques. Karsh et al. [23] presented Artificial Neural Networks (ANN) trained via the Latin hypercube to perform stochastic natural frequency analysis of functionally graded plates. They concluded that the sparsity of the output frequencies increases in accordance with the increment of the percentage of variation of input parameters. Ali et al. [24] performed natural frequency prediction analysis of Fused Deposition Modelling manufactured parts by using Artificial Neural Networks (ANN). They trained the ANN model by using the Bayesian regularization function. They concluded that the prediction error of ANN varies between 0.4% - 5.6%. Atilla et al. [25] performed free vibration and buckling analyses of laminated composite plate structures having cutouts by employing numeric and experimental methods. They used the numerical and experimental data to create an Artificial Neural Networks model to predict the first natural frequency and the critical buckling load of the composite plate with cutout. They concluded that the Artificial Neural Networks model successfully predicts the fundamental frequency and critical buckling load of the plate structure. Jayasundara et al. [26] performed damage detection in deck-type arch bridges combining modal flexibility (MMF) and modal strain energy indices (MMSE) with Artificial Neural Networks (ANN). They trained two ANN models individually via MMF and MMSE. Besides, they employed a network fusion method to improve the accuracy of damage identification. They concluded the ANN model trained by vibration data can detect, locate, and quantify damages that existed in the arch bridges. Saeed et al. [27] employed Artificial Neural Network and Multiple Neuro-Fuzzy Inference Systems (ANFIS) to identify cracks in curvilinear beams considering the natural first eight natural frequencies and frequency response. They found out that ANFIS gives better results when compared with ANN. Hakim and Abdul Razak [28] examined the damage detection of steel bridge girders by employing Artificial Neural Networks. They performed the Finite Element Method to create a dataset required for prediction. They concluded that, with a 6.8% error, ANN can determine the severity of the damage.

Yan et al. [29] performed the identification of partial cracks in supported beam structures using Back Propagating Neural Network and Support Vector Machine models. They used the optimal kernel model among Linear, Polynomial, Radial Basis Function, and Sigmoid kernels according to Mercer conditions. They concluded that the Support Vector Machine performs crack identification with smaller errors. De Fenza et al. [30] employed Artificial Neural Networks and Probability Ellipse for damage detection in composite and aluminum plates using Lamb waves. They concluded that both methods predict the damage accurately. Satpal et al. [31] used Support Vector Machine (SVM) with Radial Basis Function kernel to identify damage in aluminum beams under fixed-free and fixed-fixed boundary conditions. They employed numeric data obtained via Finite Element Analysis to train and test SVM with and without noise. They validated the results with actual experimentations and concluded that SVM accurately predicts the damage locations which makes it a promising model in structural health monitoring. Ghiasi et al. [32] used Least Square Support Vector Machine with the Littlewood-Paley wavelet kernel function to perform damage detection of four-story structures. They concluded that the accuracy of the presented model is higher than other conventional kernels. Neves et al. [33] developed a model-free damage detection method using Artificial Neural Networks for structural health monitoring of a fictitious railway bridge. They performed a two-stage process to identify whether the structure is healthy or damaged. They concluded that the proposed method is effective, especially when sensors are placed in the middle of the bridge. Kourehli [34] employed Least Squares Support Vector Machine (LS-SVM) with Gaussian Radial Basis Function kernel to detect uncertainty in cantilever plates and three-story plane frames. It is concluded in this study that the LS-SVM is sensitive to both location and severity of the damage. Hassan et al. [35] examined the rotating bending fatigue behavior of composite shafts using Artificial Neural Network (ANN) and experimental processes. They employed ANN to predict the fatigue life of the structure. They concluded that ANN successfully predict the fatigue life by a small mean square error rate of 0.0076. Ghiasi et al. [36] performed a comparative analysis considering Back-Propagation Neural Networks (BPNN), Adaptive Neural-Fuzzy Inference System (ANFIS), Radial Basis Function Neural Network (RBFN), Large Margin Nearest Neighbors(LMNN), Least-Square Support Vector Machine (LS-SVM), Extreme Learning Machine (ELM), Gaussian Process (GP), Multivariate Adaptive Regression Spline (MARS), Kriging, and Random Forest in artificial intelligence-based damage detection. They concluded that Kriging and LS-SVM models are better in location and severity of the damage. Tan et al. [37] used Artificial Neural Networks (ANN) and vibration characteristics for damage detection in steel-concrete bridges. They concluded that the model is effective since it requires only two or three vibration modes. Tran-Ngoc et al. [38] proposed an efficient Artificial Neural Network (ANN) to detect damages in bridges and beam-like structures. They increased the efficiency of the ANN model by improving the training parameters using Cuckoo Search (CS) algorithm. They concluded that ANN-CS is more accurate than ANN for damage quantification and localization.

Employing machine learning models for natural frequency evaluation is advantageous since real-world experiments are costly and time-consuming. Besides, numeric analysis methods such as the Finite Element Method, require powerful computers and software while machine learning models can be easily implemented on smaller smart devices since they are hardware and software independent. Furthermore, using the Finite Element Method or other numerical techniques requires complex mathematical equations which have to be implemented meticulously. Designing such structures using Computer-Aided Design software also takes time and requires attention since any small mistake will adversely impact the analysis results obtained via the software. On the other hand, thanks to machine learning, it may be sufficient to provide some geometrical and mechanical properties of a structure as input values to measure the static or dynamic characteristics of a structure. Besides, machine learning models can construct designs with low time consumption and high performance and help engineers or researchers to optimize a structure's design parameters. In this perspective, this study can be considered as a significant work for possible future studies that include the evaluation of static and dynamic characteristics of various structures.

All of the studies presented in Table 1 have comprehensively investigated the performance of some machine learning models for the prediction of natural frequency and damage detection, respectively. On the other hand, there are still gaps in terms of the variety of utilized machine learning methods for structural engineering problems. Besides, the effects of the thickness and boundary conditions of structures on the prediction performance of these machine learning models have not been measured yet. This study fills these gaps by using Support Vector Machine with Pearson VII Universal Function Kernel (SVM-Puk) and Radial Basis Function Regression (RBF Reg.) methods for the first time to predict the first ten natural frequencies of the very thin, thin, and thick beam structures under fixed-free, fixed-simply supported, and simply supported boundary conditions. Besides, as an ensemble learning method, Random Forest Regressor (RF) and as a conventional method, Multilayer Perceptron Regressor (MLP) have been examined.

The dataset has been obtained by utilizing the Finite Element Method employing Euler-Bernoulli and Timoshenko Beam Theories. For this purpose, a computer code was written in MATLAB to perform the finite element free vibration problem. The performance metrics (i.e., correlation coefficient, mean absolute error, root mean

Table 1. Comparison of the present study with existing literature considering various aspects

Study	Case	Frequency Range	Structure	NN	RF	SVM (RBF Kernel)	SVM (Puk Kernel)	RBF Regressor
Hakim and Abdul Razak [28]	Damage Detection	1-5	Bridge Girder	+				
Laory et al. [18]	Natural Frequency Prediction	1	Bridge	+	+	+		
Satpal et al. [31]	Damage Detection	1	Thin Aluminum Beams			+		
Ghiasi et al. [36]	Damage Detection	1-5	31-bar Planar Truss	+	+	+		
			200-bar Double-layer Grid					
He et al. [39]	Delamination Assessment	1-6	Very Thin Composite Beams	+		+		
Avcar and Saplioglu [19]	Natural Frequency Prediction	1-10	Thick Beams	+				
Atilla et al. [25]	Natural Frequency and Critical Buckling Load Prediction	1	Composite Plates with Cutouts	+				
Present Study	Natural Frequency Prediction	1-10	Very Thin, Thin, and Thick Aluminum /Steel Beams	+	+	+	+	+

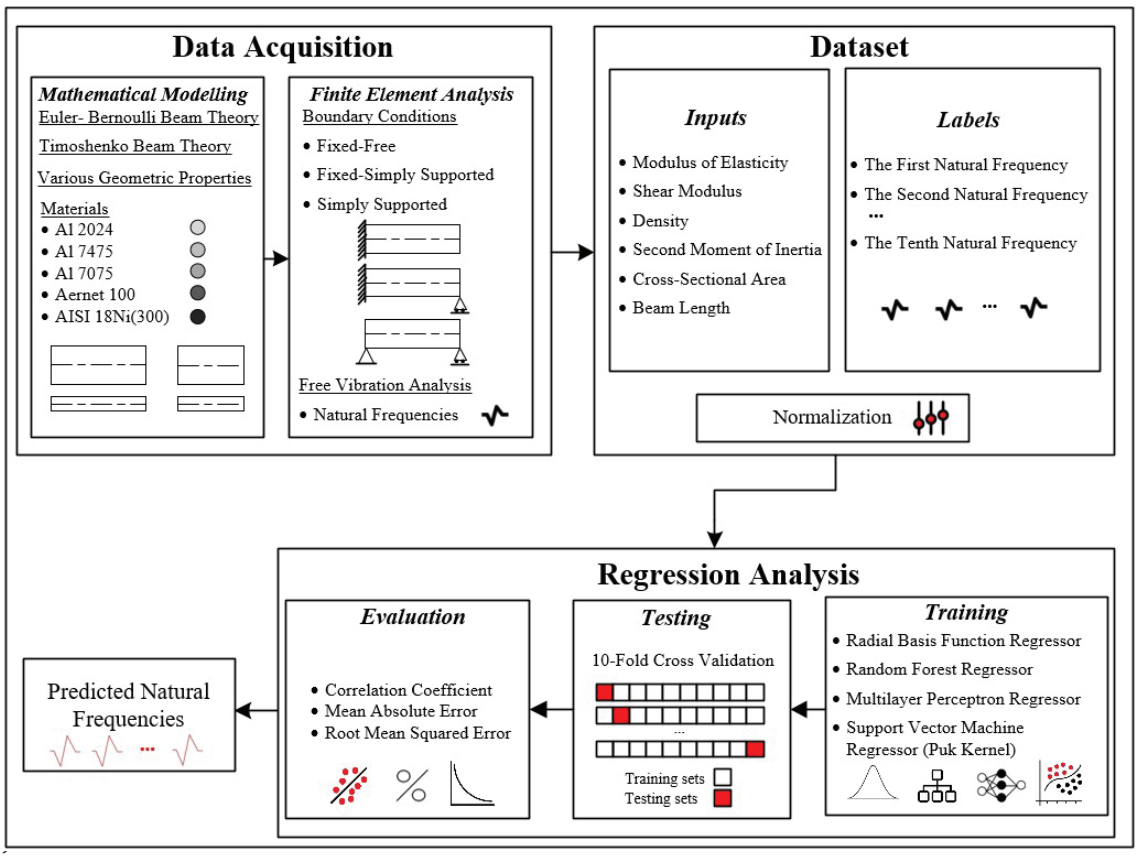

Figure 1. The prediction process of the natural frequencies using regression machine learning models.

squared error, and prediction accuracy) of the regression machine learning models have been compared considering each frequency mode, thickness, and boundary condition of the beam structure.

Figure 1 shows the general workflow of the study. The contributions of this study are presented as follows.

Proposing alternative techniques to estimate the first ten natural frequencies of very thin, thin, and thick beams under three different boundary conditions by using Radial Basis Function Regressor, Random Forest Regressor, Multilayer Perceptron Regressor, and Support Vector Machine Regressor with Pearson VII Universal Function kernel machine learning.

(i). Presenting an extensive comparison of the performance metrics of Radial Basis Function Regressor, Random Forest Regressor, Multilayer Perceptron Regressor, and Support Vector Machine with Pearson VII Universal Kernel.
(ii). Proposing the Support Vector Machine with Pearson VII Universal Kernel for the first time as a powerful alternative to other machine learning models in structural analysis.
(iii). Measuring the performance metrics of the Radial Basis Function Regressor model for the first time as another alternative model for structural engineering problems.

DATA ACQUISITION

Finite Element Modelling

The dataset used in this study has been created by employing Finite Element Vibration Analysis of different variances of aluminum and steel beam structures, shown in Figure 2. These structures have been considered under fixed-free, fixed-simply supported, and simply supported boundary conditions. Besides, Euler-Bernoulli Beam Theory and Timoshenko Beam Theory have been taken into account for stress and strain assumptions of the thin and thick beam structures, respectively. A beam element, shown in Figure 3, having two nodes and three degrees of freedom (DOF) at each node has been considered for finite element analysis. As seen in Figure 3, the considered element has two translations (u and v) and one rotation θ displacements.

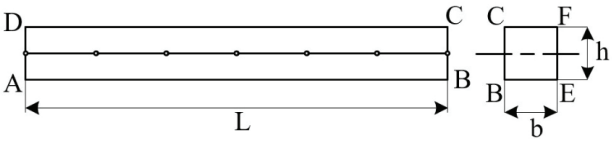

Figure 2. A beam structure.

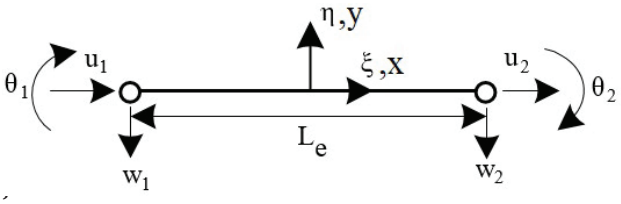

Figure 3. Beam element.

The displacement relations of the beam element are given as [40],

$$\begin{aligned} \mathrm{u} &= \mathrm{u}_0 - y\theta \\ \mathrm{w} &= \mathrm{w} \\ \theta &= \frac{2}{\mathrm{L}}\frac{\delta w}{\delta \xi} \end{aligned} \tag{1}$$

and,

$$\begin{aligned} \mathrm{u}_0 &= a_1 + a_2\xi \\ w &= a_3 + a_4\xi + \frac{a_5}{2}\xi^2 + \frac{a_6}{6}\xi^3 \\ \theta &= \frac{2}{\mathrm{L_e}}\left(a_4 + a_5\xi + \frac{a_6}{2}\xi^2\right) \end{aligned} \tag{2}$$

where a_n (n=1,2, …, 6) are the constants. The generalized displacement vector for nodal displacements can be written as

$$\mathbf{q} = [\mathrm{u}_1\ w_1\ \theta_1\ u_2\ w_2\ \theta_2] \tag{3}$$

Therefore, the displacements of any point on the beam can be evaluated as

$$\begin{bmatrix} u \\ v \\ \theta \end{bmatrix} = \boldsymbol{Nq} \tag{4}$$

where $\boldsymbol{N}$ is the shape function matrix which is,

$$\boldsymbol{N} = \begin{bmatrix} N_{m1} & 0 & 0 & N_{m2} & 0 & 0 \\ 0 & N_{bb1} & N_{bt1} & 0 & N_{bb2} & N_{bt2} \\ 0 & N_{tb1} & N_{tt1} & 0 & N_{tb2} & N_{tt2} \end{bmatrix} \tag{5}$$

and,

$$\begin{aligned} N_{mi} &= \frac{1}{2}(1 + \xi_i\xi) \\ N_{bbi} &= \frac{1}{4(1+\phi)}(\xi + \xi_i)\left(\xi_i\xi^3 + \xi + 2\xi_i(1+\phi)\right) \\ \mathrm{N_{bti}} &= \frac{L_e}{8(1+\phi)}(\xi^2 + \xi_i)\left(\xi + \xi_i(1+\phi)\right) \\ \mathrm{N_{tti}} &= \frac{1}{4(1+\phi)}(\xi + \xi_i)(3\xi - \xi_i + 2\xi_i\phi) \\ \mathrm{N_{tbi}} &= \frac{3}{2L_e(1+\phi)}(\xi_i\xi^2 + \xi_i) \end{aligned} \tag{6}$$

where ξ_i is the value of ξ at the i[th] node and,

$$\phi = \frac{12}{L_e}\left(\frac{EI}{\kappa GA}\right) \tag{7}$$

The value, φ, acts as a switch between Euler-Bernoulli and Timoshenko Beam Theories. The value is non-zero for Timoshenko beams while it is zero for Euler-Bernoulli beams [40]. The strain (U_e) and kinetic (T_e) energy equations for the beam element are given as,

$$\begin{aligned} U_e &= \frac{1}{2}EI\int_0^{L_e}\frac{\delta^2 w}{\delta\xi^2}|J|d\xi + \frac{1}{2}EA\int_0^{L_e}\frac{\delta^2 u}{\delta\xi^2}|J|d\xi + \frac{1}{2}\kappa GA\int_0^{L_e}\left(\frac{\delta w}{\delta\xi}-\theta\right)^2|J|d\xi \\ T_e &= \frac{1}{2}\rho A\int_0^{L_e}(\dot{u}^2+\dot{w}^2)|J|d\xi + \frac{1}{2}\rho I\int_0^{L_e}(\dot{\theta}^2)|J|d\xi \end{aligned} \tag{8}$$

where E and G denote the modulus of elasticity and shear modulus, respectively. ρ is the density, I represents the moment of inertia, and A is the cross-sectional area of the beam element. κ is the shear correction factor, which is considered 0.85 [40]. The energy expressions, which are given in equation (8) can be written in the matrix form as

$$\begin{aligned} U_e &= \boldsymbol{q}^T\boldsymbol{k}_e\boldsymbol{q} \\ T_e &= \boldsymbol{q}^T\boldsymbol{m}_e\boldsymbol{q} \end{aligned} \tag{9}$$

where $\boldsymbol{k}_e$ and $\boldsymbol{m}_e$ denote the element stiffness and mass matrix, respectively. The element matrices can be evaluated by performing the Gauss-Legendre numerical integration method [40].

The dynamic response of a conservative system can be obtained through Lagrange's equation of motion as

$$\boldsymbol{M}\ddot{\boldsymbol{q}} + \boldsymbol{K}\boldsymbol{q} = 0 \tag{10}$$

where ***[M]*** and ***[K]*** are the global mass and stiffness matrices of the structure. These matrices have been evaluated by assembling the element mass and element stiffness matrices obtained from Eq. (9). During the evaluation of element stiffness and mass matrices, the φ value should be considered meticulously since it is only present when the structure is thick [40]. The free vibration problem can be solved by considering Eq.(10) as an eigenvalue problem as

$$(\boldsymbol{K} - \omega^2\boldsymbol{M})\boldsymbol{q} = 0 \tag{11}$$

where ω contains the natural frequencies of the structure.

Numerical Results

The finite element vibration analyses of the beam structure under fixed-free, fixed-simply supported, and simply supported boundary conditions have been performed via a computer code written in MATLAB environment to obtain the dataset. A number of 20 elements have been considered for the Finite Element Analysis. It is considered that all structures have square cross-sections. Since the acquisition of the dataset is performed by the constructed mathematical model, it is required to check its correctness. Therefore, the validity of the finite element code is checked by conducting the free vibration analysis of fixed-free very thin, thin, and thick beams via ANSYS to check the validity of the constructed mathematical model. For this purpose, the amount of 40 of the BEAM188 element has been considered to model the same structure under the same boundary conditions in ANSYS. The scenarios considered for convergence analysis are given in Table 2. According to the convergence analysis results, given in Figure 4, the considered Finite Element Method is in close agreement with ANSYS.

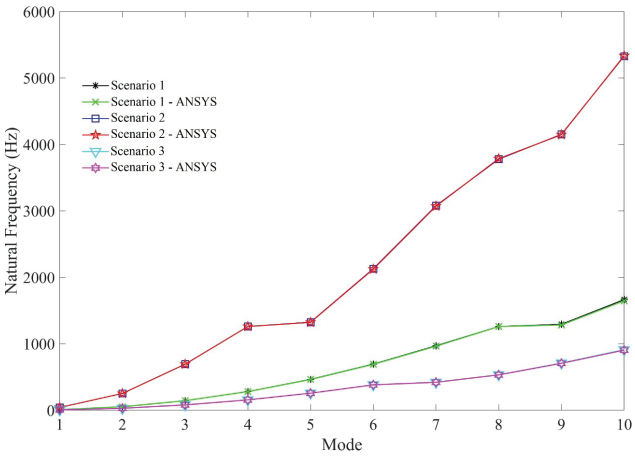

Figure 4. The convergence analysis results.

Table 2. Material properties and structural cases for convergence analysis

Material Properties			
Modulus of Elasticity (E)	72 GPa		
Shear Modulus (G)	$\frac{E}{2(1+\nu)}$		
Density (ρ)	2810 kg/m^3		
Poisson's Ratio (υ)	0.33		
Structural Cases			
Property	Scenario 1	Scenario 2	Scenario 3
Length (L)	1 m	1 m	3 m
Width (b)	0.01 m	0.05 m	0.05 m
Thickness (h)	0.01 m	0.05 m	0.05 m

In addition to convergence analysis, the transition analysis has been conducted to determine when Euler-Bernoulli (EBT) or Timoshenko Beam Theories (TBT) should be considered during the acquisition of the dataset. According to the results given in Tables 3-5, the Euler-Bernoulli Beam Theory gives more accurate results for the

thickness-length ratios smaller than 1/50 when compared with Timoshenko Beam Theory. For the thickness ratio of 1/50, the error rates vary between 0.009% and 0.704% for the Euler-Bernoulli Beam Theory based model. The upper limit of the error rate drops to 0.149% for the thickness ratio of 1/75. On the other hand, the error values of the model based on the Timoshenko Beam Theory vary between 0.009% and 1.584% for the thickness value of 1/50, whereas these values change between 0.002% and 1.737% for that of 1/75. The error percentages decrease for that model as the thickness ratio of the structure increases to 1/48, fluctuating between 0% and 1.415%. Therefore, the value of φ has been considered as zero (see Equation 7) for thickness-length ratios smaller than 1/50. In brief, the Finite Element code has employed Euler-Bernoulli Beam Theory for thickness-length ratios smaller than 1/50, while it uses

Table 3. Transition analysis results for case A

Frequency Mode	Ansys (Hz)	TBT (Hz)	Error TBT	EBT (Hz)	Error EBT
1	13.552	13.552	0.000%	13.555	0.022%
2	84.816	84.767	0.058%	84.909	0.110%
3	237.030	236.640	0.165%	237.570	0.228%
4	463.260	461.730	0.330%	465.060	0.389%
5	763.260	759.230	0.528%	767.780	0.592%
6	1049.000	1049.200	0.019%	1049.200	0.019%
7	1135.700	1127.100	0.757%	1145.200	0.836%
8	1579.000	1563.500	0.982%	1596.700	1.121%
9	2091.600	2066.300	1.210%	2122.000	1.453%
10	2671.700	2633.900	1.415%	2720.400	1.823%

Case A (L=1.2, b=h=0.025, h/L=1/48)

Table 4. Transition analysis results for case B

Frequency Mode	Ansys (Hz)	TBT (Hz)	Error TBT	EBT (Hz)	Error EBT
1	11.295	11.294	0.009%	11.296	0.009%
2	70.729	70.687	0.059%	70.769	0.057%
3	197.850	197.510	0.172%	198.060	0.106%
4	387.200	385.900	0.336%	387.840	0.165%
5	639.050	635.560	0.546%	640.560	0.236%
6	952.860	945.330	0.790%	955.920	0.321%
7	1049.000	1049.200	0.019%	1049.200	0.019%
8	1328.000	1314.000	1.054%	1333.700	0.429%
9	1763.900	1740.600	1.321%	1773.600	0.550%
10	2259.800	2224.000	1.584%	2275.700	0.704%

Case A (L=1.2, b=h=0.024, h/L=1/50)

Table 5. Transition analysis results for case C

Frequency Mode	Ansys (Hz)	TBT (Hz)	Error TBT	EBT (Hz)	Error EBT
1	9.036	9.036	0.002%	9.037	0.009%
2	56.615	56.581	0.060%	56.623	0.014%
3	158.490	158.220	0.170%	158.500	0.006%
4	310.520	309.450	0.345%	310.450	0.023%
5	513.240	510.350	0.563%	512.930	0.060%
6	766.600	760.310	0.821%	765.800	0.104%
7	1049.000	1049.200	0.019%	1049.200	0.019%
8	1070.600	1058.700	1.112%	1069.000	0.149%
9	1425.400	1405.200	1.417%	1422.400	0.210%
10	1830.900	1799.100	1.737%	1826.300	0.251%

Case C (L=1.2, b=h=0.016, h/L=1/75)

Timoshenko Beam Theory for those bigger than or equal to 1/50. The structures are denoted as *"very thin"* if their thickness-length ratio is smaller than or equal to 1/100, they are called *"thin"* if between 1/50 - 1/100, and *"thick"* if bigger than or equal to 1/50.

Dataset

The dataset created in this study comprises very thin, thin, and thick beams under fixed-free, fixed-simply supported, and simply supported boundary conditions. Table 6 gives the geometric property intervals of the considered beam structures. Table 7 presents the properties of the materials considered for each structure given in Table 6. Since all structures have a square cross-section, the dataset contains a total of 2205 structures (441 unique geometry x 5 unique materials). Besides, the dataset includes 16 attributes for each boundary condition. These attributes comprise six input and ten output values. The input parameters have been chosen as the modulus of elasticity (E), shear modulus (G), density (ρ) moment of inertia (I), cross-sectional area (A), and beam length (L). The output values are the first ten natural frequencies.

Table 6. Geometric properties of the beam structure dataset

Geometric Parameters	Initial Value	Final Value	Interval
Beam Length (L)	1 m	3 m	0.1 m
Beam Width (b)	0.01 m	0.05 m	0.002 m
Beam Thickness (h)	0.01 m	0.05 m	0.002 m

Table 7. Material properties of the beam structure dataset

Aluminum Materials			
Property	**Al 7075**	**Al 2024**	**Al 7475**
Modulus of Elasticity (GPa)	72	73.1	65
Shear Modulus (GPa)	26.9	28	24
Density (kg/m^3)	2810	2780	2520
Poisson's Ratio	0.33	0.33	0.33
Steel Materials			
Property	**Aernet 100**	**AISI 18Ni(300)**	
Modulus of Elasticity (GPa)	194	190	
Shear Modulus (GPa)	74.60	73.07	
Density (kg/m^3)	7890	8000	
Poisson's Ratio	0.3	0.3	

PREDICTION ANALYSIS

The prediction analyses have been performed by employing four different regression machine learning models, Radial Basis Function Regressor, Random Forest Regressor, Multilayer Perceptron Regressor, and Support Vector Machine Regressor with Pearson VII Universal Function Kernel (Puk) for prediction of the first ten natural frequency values of very thin, thin and thick beam structures. The experiments have been built for each machine learning model considering various boundary conditions (fixed-free, fixed-simply supported, and simply supported) and the first ten natural frequencies. Consequently, 120 experiments have been conducted, in total. To avoid overfitting and evaluating an optimal model, a 10-fold cross-validation method is employed for train-test procedures. For these procedures, input and output data are normalized between 0 and 1 considering min-max normalization. As for performance metrics, correlation coefficient, mean absolute error, root mean squared error, and prediction accuracy values have been taken into account. The *correlation coefficient* is briefly the measure of the correlation strength between two variables. The well-known indicator "R^2" is the square of the correlation coefficient indicating whether the model fits with the problem through the variance. A value close to 1 gives a high correlation (good-fit) model whereas that of close to 0 indicates low correlation. The correlation coefficient can be mathematically expressed as

$$R^2 = 1 - \frac{\sum_k (y_k - y'_k)^2}{\sum_k (y_k - \bar{y}_k)^2} \tag{12}$$

where $\sum_k (y_k - y'_k)^2$ is the sum of squares of regression or in other words, explained sum of squares and $\sum_k (y_k - \bar{y}_k)^2$ represents the total sum of squares of the outcome y.

The *mean absolute error* stands for the sum of the average absolute errors of each observation and actual output. The mean absolute error (MAE) can be calculated as

$$MAE = \frac{1}{N} \sum_k^N |y_k - y'_k| \tag{13}$$

where N is the size of the dataset, y is the actual value and y' is the predicted value. The *root mean squared error* ($RMSE$) is a quadratic metric that measures the distance between each prediction and actual value by taking the square root of the sum of the average error. $RMSE$ can be mathematically evaluated as

$$RMSE = \sqrt{\frac{1}{N} \sum_k^N (y_k - y'_k)} \tag{14}$$

The *prediction accuracy* has been evaluated by de-normalizing the predicted values and comparing them with the first ten natural frequencies of specific cases including very thin, thin, and thick beams under three boundary conditions. Since the regression analysis does not include accuracy as a performance metric, the prediction accuracy and prediction error has been evaluated as

$$Acc = 100\frac{y_k}{y_k'}$$
$$Error = 100\% - Acc \quad (15)$$

The regression machine learning models considered within this study have been explained briefly as follows.

Radial Basis Function Regressor

Radial Basis Functions are used for many purposes in many studies [19, 31, 34]. They can be employed for both classification and regression problems. In this study, the Gaussian radial basis regression function has been considered as.

$$f(x_1, x_2, \ldots, x_n) = g\left(W_o + \sum_{k=1}^{p} W_k^{-\sum_{i=1}^{m}\frac{a_i^2(x_i - c_{j,k})^2}{2\sigma_{j,k}^2}}\right) \quad (16)$$

where $x_1, x_2, \ldots, x_m$ denotes the vector of attribute values of the considered instance, *g()* is the identity function, *p* represents the amount of the basis functions, W_k *(k=0,1,2,...)* corresponds to the weight of each basis function, a_i^2 stands for the weight of the i^{th} feature, c_j is the center of the basis function and σ_j^2 is the variance of the basis function. In this study, the number of the basis functions has been chosen as five. Besides, feature weights are used and variance parameter is chosen for scale per unit. The optimal settings for feature weights and variance are evaluated on the training data by defining a local minimum of the penalized square error function [41] which is

$$L_{SE} = \left(\frac{1}{2}\sum_{k=1}^{i}\left(y_k - f(\overline{x}_k)\right)^2\right) + \left(\lambda_{rid}\sum_{j=1}^{m} W_j^2\right) \quad (17)$$

Random Forest Regressor

Random Forest Regressor is an Ensemble Learning model that combines Random Trees or Regression Trees, which grows randomly [42]. It is aimed to reduce the variance by obtaining a community including low-correlated Random Trees and averaging the outcomes. The low-correlated trees are obtained via randomization in two processes in which the first is the growth of trees by observations of randomly selected sub-dataset and the second includes splitting of the nodes of each tree by utilizing input variables of a randomly selected sub-dataset. Following the growing process of *R* amount of Random or Regression Trees using *R* sub-datasets, these trees are combined to create Random Forest. The prediction made by the Random Forest is based on bagging which can be written mathematically as

$$O(x) = \frac{1}{R}\sum_{i=1}^{R} O_i(x) + err \quad (18)$$

where *O(x)* is the prediction for a new observation called *x*, $O_i(x)$ is the evaluated prediction by using each Regression Tree, and *err* is the error.

Multilayer Perceptron (Feed-Forward Artificial Neural Network) Regressor

Multilayer Perceptron or Feed-Forward Artificial Neural Networks is a machine learning model that is used for many applications as a powerful tool [43]. The fundamental structure of this model includes input, hidden, and output layers. The output is evaluated by the summation of the combinations of the derived attributes and activation function. A simple mathematical expression for Multilayer Perceptron can be written as

$$D_m = \theta(\phi_{0n} + \phi_n^T I)$$
$$S_n = \alpha_{0n} + \alpha_n^T D$$
$$O_n(I) = S_n + err \quad (19)$$

where $D=D_1, D_2, \ldots, D_M$ is the derived attributes, which are represented by hidden layers, θ is the activation function, S_n is the linear combination of the derived attributes, $O_n(I)$ is the output as a function of the input parameters, *I*, *err* is the random error, and α and φ are the unknown parameters. In this study, the sigmoid activation function $\theta(\zeta) = 1/(1 + e^{\zeta})$ is considered since the problem is non-linear and unlike other activation functions, the sigmoid function exists only between the interval *[0, 1]* where all data is normalized. Besides, three hidden layers are employed to predict the natural frequencies of the structures. In such problems, it is important to determine the number of hidden layers. In general, one to three hidden layers is sufficient, while a big and complex dataset requires up to five hidden layers [44-46].

Support Vector Machine Regressor

Support Vector Machine Regressor or Support Vector Regression (SVR) is employed in many studies in structural engineering. The basic idea behind the SVR is reconstructing nonlinear relationships that existed in the original space to linear relationships defined in the feature space by employing a kernel function to interpret those relationships in an easy and effective way [47]. Therefore, the linear function in the feature space is given as

$$y(X) = W^T\theta(X) + b + err \quad (20)$$

where *W* denotes the weight vector, θ is the mapping function used for the transformation of the input vector *X* into the feature space, *b* is the bias constant, and *err* is the error. An SVR model is created via minimization of the objective function, which is

$$\min P(W, err) = \frac{1}{2}W^T W + \frac{1}{2}\phi\sum_{m=1}^{K} err_m^2 \quad (21)$$

where φ denotes the regularization parameter. The minimization is provided by subtracting $y_m = W^T\theta(X_m) + b + err_m$ from *P(W,err)*. This process is solved by using the Lagrangian function as

$$L(W,b,err,\gamma) = P(W,err) - \sum_{k}^{M} \gamma(W^T\beta(X_k) + b + err_k - y_k) \quad (22)$$

where γ is the Lagrange coefficient. Applying the Lagrange optimality conditions and removing weight and error gives the set of linear equations that are

$$\begin{aligned} \boldsymbol{O_M^T}\gamma &= 0 \\ \boldsymbol{O_M}b + (\psi + \phi^{-1}\boldsymbol{I_M})\gamma &= \boldsymbol{Y} \end{aligned} \quad (23)$$

where $\boldsymbol{O}_M$=*[1,1, …, 1]*$^T_{1xM}$, $\boldsymbol{I}_M$ is the *M x M* identity matrix, $\boldsymbol{Y}$=*[*y_1, y_2, …, y_M*]*^{T}, γ=*[* γ_1, γ_2, …, γ_M*]*, and ψ is the *M x M* kernel matrix expressed by the corresponding kernel function as

$$\psi = K(X_i, X_j) = \theta(X_i)^T\theta(X_j) \quad (24)$$

The kernel selection is critical since it determines the mathematical definition of the feature space and mapping function. Within the scope of this study, Pearson VII Universal Function Kernel (Puk) is employed since it is derived from a Gaussian shape, which is considered for many structural engineering applications. Therefore, the function of the Puk kernel [48] is,

$$K(X_i, X_j) = \frac{1}{\left[1 + \frac{\left(2\sqrt{\left|\left|X_i - X_j\right|\right|^2}\sqrt{2^{1\backslash\omega} - 1}\right)}{\sigma}\right]^{\omega}} \quad (25)$$

Following the solution of Eq. (19) to find the values of φ and *b*, the prediction is performed by

$$y(X) = \sum_{k=1}^{M} \phi K(X, X_k) + b \quad (26)$$

PREDICTION ANALYSES RESULTS

The prediction analyses results have been presented considering the *correlation coefficient (Cor.)*, *mean absolute error (MAE)*, and *root mean squared error (RMSE)*. Besides, the *prediction accuracy* of the machine learning models has been evaluated by de-normalizing the outputs for various test cases presented in Table 8.

For simplicity, the boundary conditions have been abbreviated. The fixed-free boundary condition is denoted as "*FF*", the fixed-simply supported boundary condition is given as "*FSS*", and the simply supported is represented by "*SS*". These abbreviations are combined with the cases given in Table 7 to indicate the case and considered boundary conditions. For instance, the structure considered in Case B1 under fixed-free boundary conditions is denoted as "*FF-B1*".

Table 8. Considered beam cases to test the employed machine learning techniques

Case ID	B1	B2	B3
Beam Length (L)	1.2 m	2 m	2.8 m
Beam Width (b)	0.04 m	0.024 m	0.014 m
Beam Thickness (h)	0.04 m	0.024 m	0.014 m
Material	Al 7075	AISI 18Ni(300)	Al 2024

The performance of the machine learning models has been measured considering (i) the thickness-length ratio and corresponding theory, (ii) boundary conditions, and (iii) natural frequencies. The kernel of the support vector machine has been chosen as Pearson VII Universal Function Kernel (Puk) since it outperforms the Radial Basis Kernel (RBF), which is mostly employed for structural engineering problems in which Support Vector Machine has been considered. For instance, considering the prediction performance of the fundamental natural frequencies of the *FF-B1*, *FF-B2*, and *FF-B3* structures, the correlation factor, mean absolute error, and root mean squared error of RBF has been evaluated as 0.8944, 0.0531, and 0.0984, respectively while these values have been evaluated as 0.9997, 0.0017, and 0.0047 for Puk. Besides the prediction accuracy of RBF is considerably off when compared with that of Puk. The prediction error rates of RBF for the first natural frequency of the *FF-B1, FF-B2*, and *FF-B3* cases have been obtained as 35%, 16%, and 75%, respectively, whereas the prediction error rates of Puk for these cases have been evaluated as 0.68%, 0.53%, and 4.48%, respectively.

Tables 9 - 11 give the statistical performance metrics results of Radial Basis Function Regressor (RBF Reg), Random Forest Regressor (RF), Multilayer Perceptron Regressor (MLP), and Support Vector Machine Regressor with Puk kernel (SVM-Puk) considering the randomly selected testing data under *FF*, *FSS*, and *SS* boundary conditions, respectively. The highest correlation factor values, the lowest mean absolute errors, and the lowest root mean squared errors are highlighted with bold font.

It is seen from Tables 9-11 that the best metrics have been obtained for SVM-Puk. The correlation coefficients of all machine learning models are above 0.99, which proves that the created models have a good fit for the prediction problem. The average mean absolute error and root mean squared error values indicate that RF and SVM-Puk are

Table 9. Statistical performance metrics results for *FF* (Avg.: Average)

Mode	RBF Reg.			RF			MLP			SVM-Puk		
	Cor.	***MAE***	***RMSE***	***Cor.***	***MAE***	***RMSE***	***Cor.***	***MAE***	***RMSE***	***Cor.***	***MAE***	***RMSE***
1	0.9995	0.0042	0.0059	0.9992	0.0048	0.0081	0.9986	0.0067	0.0094	**0.9997**	**0.0017**	**0.0047**
2	0.9991	0.0048	0.0077	0.9991	0.005	0.0083	0.9986	0.0067	0.0094	**0.9997**	**0.0017**	**0.0046**
3	0.9994	0.0042	0.006	0.9991	0.005	0.0085	0.9986	0.0067	0.0094	**0.9997**	**0.0017**	**0.0047**
4	0.9995	0.0045	0.0065	0.9991	0.0055	0.0091	0.9987	0.0074	0.0103	**0.9998**	**0.0016**	**0.0036**
5	0.9988	0.0074	0.0113	0.9994	0.0056	0.009	0.9962	0.0152	0.0204	**0.9995**	**0.0027**	**0.0072**
6	0.9973	0.0087	0.0131	0.9992	0.0048	0.0081	0.994	0.0147	0.0195	**0.9994**	**0.0029**	**0.0066**
7	0.9979	0.008	0.0112	0.9991	0.0048	0.0083	0.9972	0.0104	0.0132	**0.9993**	**0.0030**	**0.0066**
8	0.9988	0.0077	0.0102	0.9992	0.0057	0.0093	0.9976	0.0118	0.0148	**0.9997**	**0.0029**	**0.0053**
9	0.9986	0.0073	0.0108	**0.9993**	0.0052	**0.0086**	0.9948	0.0149	0.0211	0.999	**0.0039**	0.0093
10	0.9978	0.0085	0.0124	0.9992	0.0049	0.0084	0.995	0.0138	0.0187	**0.9994**	**0.0034**	**0.0068**
Avg.	0.9987	0.0065	0.0095	0.9992	0.0051	0.0086	0.9969	0.0108	0.0146	**0.9995**	**0.0026**	**0.0059**

Table 10. Statistical performance metrics results for *FSS* (Avg.: Average)

Mode	RBF Reg.			RF			MLP			SVM-Puk		
	Cor.	***MAE***	***RMSE***	***Cor.***	***MAE***	***RMSE***	***Cor.***	***MAE***	***RMSE***	***Cor.***	***MAE***	***RMSE***
1	0.9995	0.004	0.0057	0.999	0.005	0.0087	0.9986	0.0067	0.0094	**0.9997**	**0.0016**	**0.0047**
2	0.9994	0.0043	0.0064	0.9991	0.005	0.0084	0.9986	0.0067	0.0094	**0.9997**	**0.0017**	**0.0047**
3	0.9996	0.0038	0.0053	0.9991	0.005	0.0084	0.9986	0.0067	0.0094	**0.9997**	**0.0016**	**0.0046**
4	0.9993	0.0066	0.0094	0.9993	0.0061	0.0098	0.9978	0.0121	0.0165	**0.9998**	**0.0024**	**0.0049**
5	0.9972	0.0091	0.0137	0.9992	0.0049	0.0084	0.9941	0.0157	0.0203	**0.9994**	**0.0029**	**0.0066**
6	0.9978	0.0079	0.0114	**0.9992**	0.0047	0.0081	0.996	0.012	0.0156	**0.9992**	**0.0030**	**0.0069**
7	0.9986	0.008	0.0104	0.9992	0.0056	0.0091	0.9967	0.0127	0.0161	**0.9997**	**0.0028**	**0.0053**
8	0.9986	0.0071	0.0113	**0.9993**	0.0055	0.0089	0.9959	0.0139	0.0193	0.9991	**0.0038**	**0.0093**
9	0.9981	0.0081	0.0116	0.9992	0.0049	0.0083	0.9936	0.0159	0.0213	**0.9994**	**0.0033**	**0.0066**
10	0.9983	0.0081	0.0122	0.9992	0.0057	0.0093	0.9967	0.0124	0.017	**0.9996**	**0.0034**	**0.0062**
Avg.	0.9986	0.0067	0.0097	0.9992	0.0052	0.0087	0.9967	0.0115	0.0154	**0.9995**	**0.0027**	**0.0060**

Table 11. Statistical performance metrics results for *SS* (Avg.: Average)

Mode	RBF Reg.			RF			MLP			SVM-Puk		
	Cor.	***MAE***	***RMSE***	***Cor.***	***MAE***	***RMSE***	***Cor.***	***MAE***	***RMSE***	***Cor.***	***MAE***	***RMSE***
1	0.9995	0.0041	0.0057	0.9991	0.005	0.0084	0.9986	0.0067	0.0094	**0.9997**	**0.0016**	**0.0047**
2	0.9994	0.0042	0.0061	0.9991	0.0049	0.0083	0.9986	0.0067	0.0094	**0.9997**	**0.0017**	**0.0047**
3	0.9995	0.004	0.0057	0.9991	0.005	0.0084	0.9986	0.0067	0.0094	**0.9997**	**0.0016**	**0.0047**
4	0.9993	0.0063	0.0086	0.9993	0.0062	0.0097	0.9986	0.009	0.0123	**0.9998**	**0.0021**	**0.0046**
5	0.9962	0.0107	0.0169	0.9993	0.0048	0.008	0.9925	0.0178	0.0237	**0.9995**	**0.0030**	**0.0064**
6	0.9979	0.0074	0.0112	0.9991	0.0047	0.0082	0.9951	0.0128	0.0173	**0.9993**	**0.0030**	**0.0069**
7	0.9986	0.0075	0.0099	0.9991	0.0051	0.0086	0.9972	0.0108	0.0139	**0.9996**	**0.0028**	**0.0056**
8	0.999	0.0071	0.0097	0.9993	0.0057	0.0092	0.9979	0.0105	0.0143	**0.9995**	**0.0034**	**0.0068**
9	0.9983	0.0079	0.0114	0.9993	0.0049	0.0079	0.9923	0.0177	0.024	**0.9995**	**0.0033**	**0.0064**
10	0.9983	0.0076	0.0114	0.9992	0.0054	0.009	0.9961	0.0128	0.0174	**0.9995**	**0.0035**	**0.0065**
Avg.	0.9986	0.0067	0.0097	0.9992	0.0052	0.0086	0.9966	0.0112	0.0151	**0.9996**	**0.0026**	**0.0057**

Table 12. Prediction accuracy results of the machine learning models for *FF-B1* (Avg. :Average)

Mode	Actual	RBF Reg.		RF		MLP		SVM-Puk	
		Predicted	*Err. (%)*	*Predicted*	*Err. (%)*	*Predicted*	*Err. (%)*	*Predicted*	*Err. (%)*
1	22.709	22.99872	1.28%	22.62288	**0.38%**	22.94784	1.05%	22.86352	0.68%
2	142.130	141.7774	0.25%	142.1563	**0.02%**	143.6329	1.06%	142.8673	0.52%
3	397.160	389.8571	1.84%	389.5369	1.92%	401.3874	1.06%	399.7805	**0.66%**
4	775.970	775.6896	**0.04%**	768.1638	1.01%	807.6732	4.09%	781.6367	0.73%
5	1054.800	1067.067	1.16%	1064.306	0.90%	1044.449	0.98%	1058.924	**0.39%**
6	1277.900	1252.991	1.95%	1265.330	0.98%	1277.557	**0.03%**	1280.086	0.17%
7	1900.300	1928.809	1.50%	1903.447	0.17%	1906.769	0.34%	1911.473	0.59%
8	2640.300	2668.179	**1.06%**	2604.605	1.35%	2688.703	1.83%	2671.011	1.16%
9	3171.000	3212.051	1.29%	3189.941	**0.60%**	3291.221	3.79%	3217.831	1.48%
10	3494.800	3666.098	4.90%	3441.424	1.53%	3565.216	2.01%	3493.057	**0.05%**
Avg.			1.53%		0.89%		1.62%		**0.64%**

Table 13. Prediction accuracy results of the machine learning models for *FF-B2* (Avg. :Average)

Mode	Actual	RBF Reg.		RF		MLP		SVM-Puk	
		Predicted	*Err. (%)*	*Predicted*	*Err. (%)*	*Predicted*	*Err. (%)*	*Predicted*	*Err. (%)*
1	4.723	4.598047	2.65%	4.747752	**0.52%**	4.2927	9.11%	4.748146	0.53%
2	29.578	28.02578	5.25%	29.8816	1.03%	26.87681	9.13%	29.64805	**0.24%**
3	82.732	81.79053	1.14%	83.23424	**0.61%**	75.15606	9.16%	83.36932	0.77%
4	161.88	158.024	2.38%	163.1512	0.79%	147.895	8.64%	162.4824	**0.37%**
5	267.1	261.2125	2.20%	273.132	2.26%	240.5566	9.94%	266.6485	**0.17%**
6	398.16	416.2829	4.55%	401.8567	0.93%	414.9792	4.22%	397.5558	**0.15%**
7	554.81	532.6539	3.99%	555.8012	**0.18%**	527.1096	4.99%	555.2045	**0.07%**
8	609.33	583.827	4.19%	615.9853	1.09%	594.4284	2.45%	608.9149	**0.07%**
9	736.87	742.6907	0.79%	749.7833	**1.75%**	629.2094	14.61%	734.511	**0.32%**
10	944.2	918.6864	2.70%	951.629	0.79%	800.4082	15.23%	940.8858	**0.35%**
Avg.			2.98%		0.99%		8.75%		**0.30%**

Table 14. Prediction accuracy results of the machine learning models for *FF-B3* (Avg. :Average)

Mode	Actual	RBF Reg.		RF		MLP		SVM-Puk	
		Predicted	*Err. (%)*	*Predicted*	*Err. (%)*	*Predicted*	*Err. (%)*	*Predicted*	*Err. (%)*
1	1.465	1.551948	5.94%	1.489847	1.70%	1.455635	**0.64%**	1.399404	4.48%
2	9.18	9.935605	8.23%	9.273723	1.02%	9.117408	**0.68%**	8.981916	2.16%
3	25.7	28.58218	11.21%	25.52818	**0.67%**	25.50368	0.76%	25.38764	1.22%
4	50.35	54.61441	8.47%	50.97032	**1.23%**	57.14192	13.49%	48.64671	3.38%
5	83.211	91.51653	9.98%	85.7839	3.09%	74.48148	10.49%	81.90109	**1.57%**
6	124.28	121.3863	2.33%	123.4173	**0.69%**	133.9821	7.81%	120.9892	2.65%
7	173.55	162.386	6.43%	175.8086	**1.30%**	134.9531	22.24%	168.6191	2.84%
8	231.06	272.3136	17.85%	234.0916	**1.31%**	241.6475	4.58%	224.3742	2.89%
9	296.85	308.7233	4.00%	296.054	**0.27%**	350.4705	18.06%	294.8535	0.67%
10	370.99	358.464	3.38%	373.1357	0.58%	433.8045	16.93%	371.3326	**0.09%**
Avg.			7.78%		**1.19%**		9.57%		2.20%

more suitable than RBF Reg and MLP since the error values of RF and SVM-Puk are much lower than those of RBF Reg and MLP. The statistical performance metrics are essential since they provide insight and significant information about the fitting performance of machine learning models. However, the predicted observations have to be taken into account to evaluate the realistic performance of a model. Tables 12-14 give the predicted observations for the randomly selected testing data and corresponding errors of the considered machine learning algorithms for fixed-free boundary conditions. The lowest prediction error of the model is indicated with the bold font for each vibration mode.

According to the results given in Tables 12-14, the SVM-Puk model has the lowest prediction error for *FF-B1* and *FF-B2* cases (0.64% and 0.30%) while the RF model has shown the best performance for the *FF-B3* case by 1.19% error. It is seen that each machine learning model has made accurately predicted almost all-natural frequencies of the *FF-B1* structure. However, for both RBF Reg. and MLP, the average prediction error rates have increased for *B2* to 2.98% and 8.75% and for *B3* to 7.78% and 9.57%, respectively. This indicates that these models are effective for thick beams since the average prediction error values of these models are 1.53% for RBF Reg. and 1.62% for MLP considering the thick structure, *B1*. On the other hand, SVM-Puk and RF models give accurate predictions in all cases, although their performances are slightly affected by the thickness-length ratio. In general, the prediction error rates have decreased for higher thickness-length ratios. The RF model predicted the first ten natural frequencies of the *FF-B3* case by an average error rate of 1.19% while the average prediction error has diminished to 0.99% for the *FF-B2* case and 0.89% for the *FF-B1* case. The average prediction error of SVM-Puk performed a prediction of the first ten natural frequencies of the *FF-B1* structure by an average error of 0.64%. This average prediction error rate diminished for the *FF-B2* structure to 0.30% and increased for the *FF-B3* structure to 2.20%. Considering the RF model, it is seen that the average accuracy values are evaluated by 0.89% for the *FF-B1* case, 0.99% for *FF-B2*, and 1.29% for the *FF-B3* structure.

Tables 15-17 present the predictions, actual values and corresponding errors of the four different regression machine learning algorithms for fixed-simply supported *FSS* boundary conditions considering the randomly selected testing data. The lowest prediction error of the model is indicated with the bold font for each vibration mode.

It is seen from Tables 15-17 that the SVM-Puk model has the best performance for *FF-B1* and *FF-B2* cases by 0.82% and 0.41% errors, while the RF model has the lowest prediction error for the *FF-B3* case (1.32%). A similar interpretation made for the prediction results of the first ten natural frequencies of *FF* structure can be made for the *FSS* case. The prediction performance slightly changes for all machine learning models when compared to *FF*. Among those models, the most considerable changes in terms of prediction accuracy have occurred for RBF Reg. whose average prediction error has been decreased by 1.40% for the case *FSS-B3*, and for MLP whose performance has been improved by 1.56% for the case *FSS-B2*. Just as for the *FF* case, the prediction accuracy has generally increased as the thickness-length ratio increases. The average error values for the RBF Reg. model are 1.20% for the *FSS-B1* case, 2.48% for *FSS-B2*, and 6.38% for the *FSS-B3* structure. For the MLP model, these values are 2.01%, 7.19%, and 9.40%, respectively. The average prediction error values of the RF model are 1.04% for *FSS-B1*, 1.36% for *FSS-B2*, and 1.32% for the *FSS-B3* structure.

Table 15. Prediction accuracy results of the machine learning models for *FSS-B1* (Avg. :Average)

Mode	Actual	RBF Reg.		RF		MLP		SVM-Puk	
		Predicted	*Err. (%)*	*Predicted*	*Err. (%)*	*Predicted*	*Err. (%)*	*Predicted*	*Err. (%)*
1	99.55	98.7976	0.76%	97.85503	1.70%	100.5944	1.05%	100.0921	**0.54%**
2	322.14	321.3988	**0.23%**	314.5614	2.35%	325.5367	1.05%	324.1209	0.61%
3	670.57	684.8276	2.13%	663.8414	1.00%	677.6728	1.06%	674.629	**0.61%**
4	1054.8	1065.107	0.98%	1060.999	0.59%	1064.299	0.90%	1060.779	**0.57%**
5	1143.1	1177.854	3.04%	1140.283	0.25%	1123.319	1.73%	1142.089	**0.09%**
6	1737.5	1756.746	1.11%	1716.397	1.21%	1736.361	**0.07%**	1747.891	0.60%
7	2451	2438.888	**0.49%**	2420.953	1.23%	2555.964	4.28%	2471.857	0.85%
8	3171	3245.146	2.34%	3198.22	**0.86%**	3250.935	2.52%	3210.272	1.24%
9	3280.6	3285.188	**0.14%**	3314.436	1.03%	3473.595	5.88%	3339.94	1.81%
10	4223.2	4189.96	0.79%	4229.196	**0.14%**	4158.989	1.52%	4276.536	1.26%
Avg.			1.20%		1.04%		2.01%		**0.82%**

Table 16. Prediction accuracy results of the machine learning models for *FSS-B2* (Avg. :Average)

Mode	Actual	RBF Reg.		RF		MLP		SVM-Puk	
		Predicted	*Err. (%)*	*Predicted*	*Err. (%)*	*Predicted*	*Err. (%)*	*Predicted*	*Err. (%)*
1	20.701	20.19235	2.46%	20.71169	**0.05%**	18.81112	9.13%	20.81425	0.55%
2	67.021	67.37737	0.53%	68.22448	1.80%	60.8737	9.17%	67.20129	**0.27%**
3	139.64	134.4552	3.71%	137.9326	1.22%	126.7644	9.22%	140.2462	**0.43%**
4	238.37	229.3974	3.76%	239.971	0.67%	232.9104	2.29%	238.4767	**0.04%**
5	362.98	365.4822	0.69%	366.7592	1.04%	370.6424	2.11%	364.2867	**0.36%**
6	513.26	500.0339	2.58%	518.6542	1.05%	497.7832	3.02%	517.8904	**0.90%**
7	609.33	605.5353	0.62%	615.2939	0.98%	615.754	1.05%	608.6666	**0.11%**
8	689	708.1252	2.78%	697.3252	1.21%	584.3548	15.19%	693.6794	**0.68%**
9	890.05	925.0864	3.94%	915.2962	2.84%	723.226	18.74%	883.7839	**0.70%**
10	1116.4	1157.847	3.71%	1146.566	2.70%	1138.442	1.97%	1115.508	**0.08%**
Avg.			2.48%		1.36%		7.19%		**0.41%**

Table 17. Prediction accuracy results of the machine learning models for *FSS-B3* (Avg. :Average)

Mode	Actual	RBF Reg.		RF		MLP		SVM-Puk	
		Predicted	*Err. (%)*	*Predicted*	*Err. (%)*	*Predicted*	*Err. (%)*	*Predicted*	*Err. (%)*
1	6.424	6.970579	8.51%	6.541047	1.83%	6.380304	**0.68%**	6.279705	2.24%
2	20.814	22.5584	8.38%	21.14222	1.58%	20.65785	**0.75%**	20.01794	3.82%
3	43.416	42.46771	2.18%	42.92019	1.14%	43.04837	**0.85%**	41.84486	3.62%
4	74.227	76.56476	3.15%	75.70274	**1.99%**	62.85615	15.32%	73.50398	0.97%
5	113.24	130.1967	14.97%	114.6331	**1.23%**	130.2786	15.05%	110.9761	2.00%
6	160.46	149.8426	6.62%	160.4997	**0.02%**	115.6219	27.94%	159.0938	0.85%
7	215.92	201.8659	6.51%	222.5772	3.08%	233.9427	8.35%	210.0093	**2.74%**
8	279.64	274.5886	1.81%	282.2142	0.92%	293.6118	5.00%	278.3035	**0.48%**
9	351.69	347.8065	1.10%	355.0647	**0.96%**	405.2811	15.24%	355.7157	1.14%
10	432.18	386.4051	10.59%	434.067	**0.44%**	411.2843	4.83%	398.3442	7.83%
Avg.			6.38%		**1.32%**		9.40%		2.57%

Considering the SVM-Puk model, these values are 0.82%, 0.41%, and 2.57%, respectively.

Tables 18-20 present the predictions, actual values, and corresponding errors of the four different regression machine learning algorithms for simply supported boundary conditions considering the randomly selected testing data. The lowest prediction error of the model is indicated with the bold font for each vibration mode.

It is seen from Tables 18-20 that the SVM-Puk model has the lowest prediction error for *FF-B1* and *FF-B2* cases (0.67% and 0.65%), while the RF model has the best performance for the *FF-B3* case by 1.32% error. The prediction performance metrics that have been evaluated for *SS* cases slightly change for almost all machine learning models when compared with the *FSS* cases. The most considerable differences have occurred for MLP, whose average prediction error decrease by 1.05% for the case *SS-B2*, and 3.24% for the case *SS-B3*. The performance of machine learning models has been generally higher for thicker structures. The average prediction error values of the RBF Reg. model are 1.30% for the *SS-B1* case, 2.52% for *SS-B2*, and 6.63% for the *SS-B3* structure. Considering the MLP model, these values are 1.72%, 6.14%, and 6.16%, respectively. The average error values for the RF model are 0.86% for *SS-B1*, 1.12% for *SS-B2*, and 1.35% for *SS-B3* structure. For the SVM-Puk model, these values are 0.67%, 0.65%, and 2.73%, respectively.

Evaluating all results given in Tables 11-20 considering the thickness-length ratio of the structure indicates that the SVM-Puk model gives the most accurate predictions for the *B1* and *B2* cases under *FF*, *FSS*, and *SS* boundary conditions. The average accuracy values of the SVM-Puk

Table 18. Prediction accuracy results of the machine learning models for *SS-B1* (Avg. :Average)

Mode	Actual	RBF Reg.		RF		MLP		SVM-Puk	
		Predicted	*Err. (%)*	*Predicted*	*Err. (%)*	*Predicted*	*Err. (%)*	*Predicted*	*Err. (%)*
1	63.73	64.59937	1.36%	63.45709	**0.43%**	64.39938	1.05%	64.14834	0.66%
2	254.57	260.0077	2.14%	248.4182	2.42%	257.2664	1.06%	256.1416	**0.62%**
3	571.5	585.2803	2.41%	570.6218	**0.15%**	577.597	1.07%	574.3468	0.50%
4	1012.9	1008.136	**0.47%**	1019.68	0.67%	980.0798	3.24%	1002.652	1.01%
5	1054.8	1061.455	0.63%	1059.85	**0.48%**	1051.136	0.35%	1059.817	**0.48%**
6	1576.5	1575.145	0.09%	1577.413	**0.06%**	1557.179	1.23%	1587.823	0.72%
7	2259.7	2280.248	0.91%	2230.153	1.31%	2355.098	4.22%	2273.851	**0.63%**
8	3059.5	2990.019	2.27%	3013.205	1.51%	2989.894	2.28%	3023.134	**1.19%**
9	3171	3211.686	1.28%	3190.24	0.61%	3247.579	2.41%	3166.888	**0.13%**
10	3972.8	3916.197	1.42%	3932.683	1.01%	3984.937	0.31%	4002.951	**0.76%**
Avg.			1.30%		0.86%		1.72%		**0.67%**

Table 19. Prediction accuracy results of the machine learning models for *SS-B2* (Avg. :Average)

Mode	Actual	RBF Reg.		RF		MLP		SVM-Puk	
		Predicted	*Err. (%)*	*Predicted*	*Err. (%)*	*Predicted*	*Err. (%)*	*Predicted*	*Err. (%)*
1	13.256	12.90514	2.65%	13.24938	**0.05%**	12.04746	9.12%	13.32911	0.55%
2	52.986	53.91493	1.75%	52.84378	0.27%	52.36531	1.17%	52.99757	**0.02%**
3	119.08	116.0069	2.58%	120.4249	1.13%	108.1688	9.16%	120.1463	**0.90%**
4	211.38	199.2251	5.75%	212.5976	0.58%	201.4007	4.72%	212.5078	**0.53%**
5	329.67	326.8634	0.85%	340.9062	3.41%	314.4625	4.61%	331.8493	**0.66%**
6	473.73	498.2249	5.17%	481.7362	1.69%	468.8363	1.03%	472.4063	**0.28%**
7	609.33	607.1535	0.36%	615.0826	0.94%	607.0502	0.37%	609.3277	**0.00%**
8	643.37	652.404	1.40%	642.5943	**0.12%**	633.4077	1.55%	660.1905	2.61%
9	838.42	819.2894	2.28%	847.598	1.09%	663.0391	20.92%	830.9912	**0.89%**
10	1058.8	1084.768	2.45%	1079.279	1.93%	966.4437	8.72%	1059.665	**0.08%**
Avg.			2.52%		1.12%		6.14%		**0.65%**

Table 20. Prediction accuracy results of the machine learning models for *SS-B3* (Avg. :Average)

Mode	Actual	RBF Reg.		RF		MLP		SVM-Puk	
		Predicted	*Err. (%)*	*Predicted*	*Err. (%)*	*Predicted*	*Err. (%)*	*Predicted*	*Err. (%)*
1	4.1122	4.453032	8.29%	4.064699	1.16%	4.085515	**0.65%**	3.95292	3.87%
2	16.447	16.58876	0.86%	16.51598	**0.42%**	16.33212	0.70%	15.92152	3.20%
3	36.999	36.14376	2.31%	37.76693	2.08%	36.71105	**0.78%**	36.25738	2.00%
4	65.762	75.03942	14.11%	66.83969	**1.64%**	70.98043	7.94%	63.77482	3.02%
5	102.73	109.5017	6.59%	105.6112	2.80%	124.0949	20.80%	101.014	**1.67%**
6	147.91	139.235	5.87%	149.042	**0.77%**	134.3855	9.14%	145.7377	1.47%
7	201.32	186.6648	7.28%	200.1847	**0.56%**	203.5079	1.09%	197.6184	1.84%
8	262.98	279.62	6.33%	264.3827	**0.53%**	269.2584	2.39%	259.1527	1.46%
9	332.97	369.1922	10.88%	336.3276	**1.01%**	388.1859	16.58%	338.0006	1.51%
10	411.37	395.9507	3.75%	421.8041	2.54%	417.8999	**1.59%**	381.4503	7.27%
Avg.			6.63%		**1.35%**		6.16%		2.73%

for *FF-B1*, FF-B2, FSS-B1, FSS-B2, SS-B1, and SS-B2 are 99.36%, 99.70%, 99.18%, 99.59%, 99.33%, and 99.35%, respectively. On the other hand, RF is the best model for the *B3* case under all boundary conditions. The average prediction accuracy values of the RF model are 98.81% for *FF-B3*, 98.68% for *FSS-B3*, and 98.65% for *SS-B3* cases. The prediction accuracy values of the RBF Reg. and MLP models are not high as those of SVM-Puk and RF models. Nevertheless, the predictions made by the RBF Reg. and MLP models are also accurate. The prediction accuracy values of those models change between 91.43% (MLP for the case *FF-B3*) and 98.80% (RBF Reg. for the case *FSS-B1*) depending on the boundary conditions and dimensions of the structure.

Although the evaluation of the first ten natural frequencies is significant, predicting the fundamental frequency of a structure is critical since in most cases, the phenomenon called resonance can be observed in the structures at their first natural frequency. Therefore, considering the predictions of the fundamental natural frequencies indicate that the most accurate predictions have been performed by MLP for very thin (B3) structures by an average accuracy value of 99.34%. On the other hand, the RF model predicts the fundamental frequencies of thick (B1) and thin (B2) structures by an average accuracy value of 99.48%.

Comparing the sensitivity of the models to the structure's thickness shows that RF is the most robust model against the differences in thickness-length ratio since the error rates change in a small interval, which is between 0.89% and 1.35%. On the other hand, SVM-Puk is also a strong model for thick and thin structures, while the performance has slightly decreased for the very thin beams under all boundary conditions. The prediction error rates of RBF Reg. are acceptable for thick structures, while the performance has been decreased for the thin and specifically for the very thin beam structures. MLP gives a good prediction performance for the thick structure, whereas its prediction performance drastically for thin and very thin beams. The most sensitive model is the MLP model since the error rates vary in a large interval, which is between 1.62% and 9.57%. This is because the MLP technique is sensitive to feature scaling, such as normalization. Another reason is the existence of non-convex loss functions where more than a single local minimum can be observed. This causes the initialization of the weights randomly which resulted in differences in accuracy values for each predicting case.

Figures 5 and 6 show the average prediction error of the regression models for each natural frequency of the *B1*, *B2*, and *B3* structures regardless of their boundary conditions. Figures 5 and 6 indicate that the RBF Regressor and MLP are sensitive to the length-thickness ratio since their prediction accuracies have been adversely affected as the structures become thinner. On the other hand, the performance metrics of the SVM-Puk and RF have not been considerably affected by the structure's thickness. Therefore, it can be concluded that the SVM-Puk and RF are robust against the length-thickness ratio of the structure.

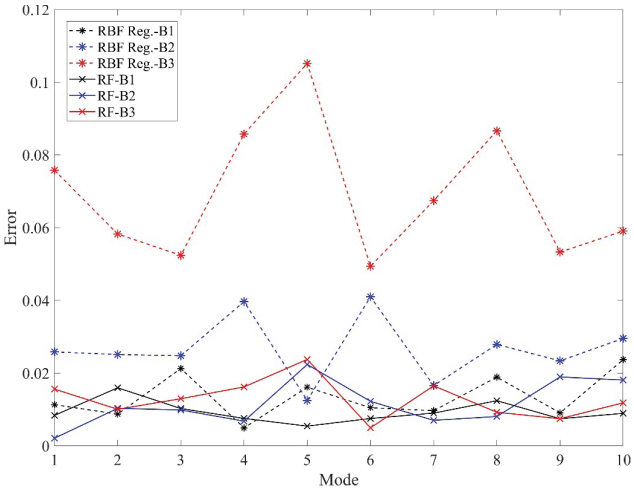

Figure 5. Average prediction error of the RBF Reg. and RF for each vıbratıon mode of B1, B2, and B3 beams.

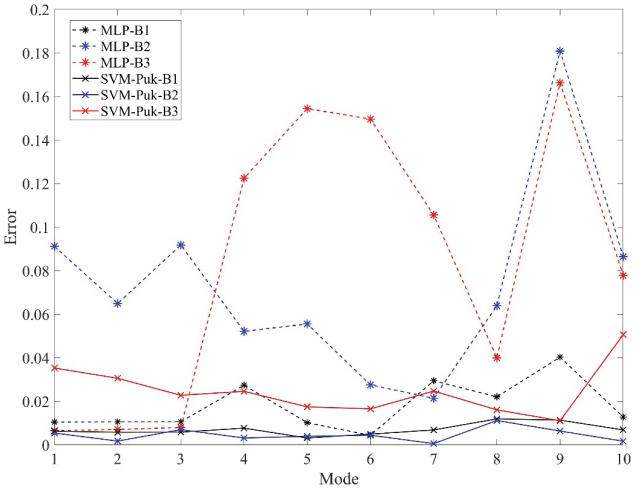

Figure 6. Average prediction error of the MLP and SVM-Puk for each vibration mode of B1, B2, and B3 beams.

Figures 7 and 8 show the boundary condition effects on the performance of the regression machine learning models considering the average error of each prediction for each vibration mode of the beam structure regardless of their thickness-length ratio.

It is seen from Figures 7 and 8 that the prediction accuracies of the SVM-Puk and RF are robust and have not been considerably affected by the change of boundary conditions. RBF Reg. has been slightly affected by different boundary conditions. On the other hand, the prediction performance of RBF Reg. can be ordered from the

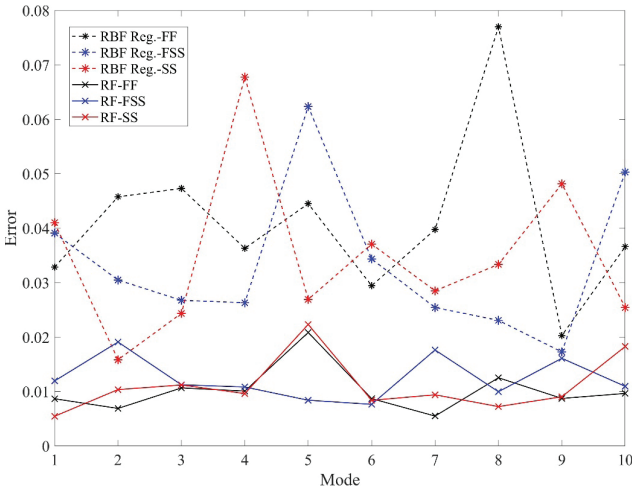

Figure 7. Average prediction error of the RBF Reg. and RF for each vibration mode of FF, FSS, and SS beams.

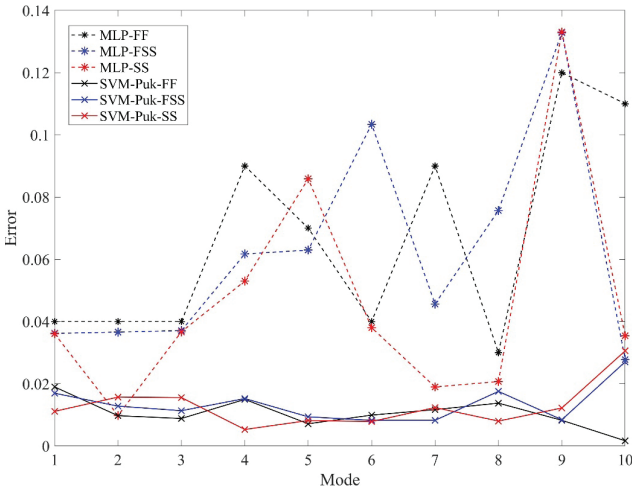

Figure 8. Average prediction error of the MLP and SVM-Puk for each vibration mode of FF, FSS, and SS beams.

highest to the lowest as *SS*, *FSS*, and *FF*, respectively. MLP is the most sensitive model whose prediction performance has been affected by the boundary condition, especially for the *B2* and *B3* cases. Overall, the performance of MLP can be ordered from the highest to the lowest as, *SS*, *FSS*, and *FF*, respectively.

Figure 9 shows the average prediction error of the regression machine learning models per vibration mode regardless of thickness-length ratio and boundary conditions. It is seen from Figure 9 that the SVM-Puk and RF models have shown the best prediction performance with error rates varying between 1% and 2%. The overall error rates of RBF Reg. change between 3% and 4%, while the average error rates differ between 4% - 12% for MLP.

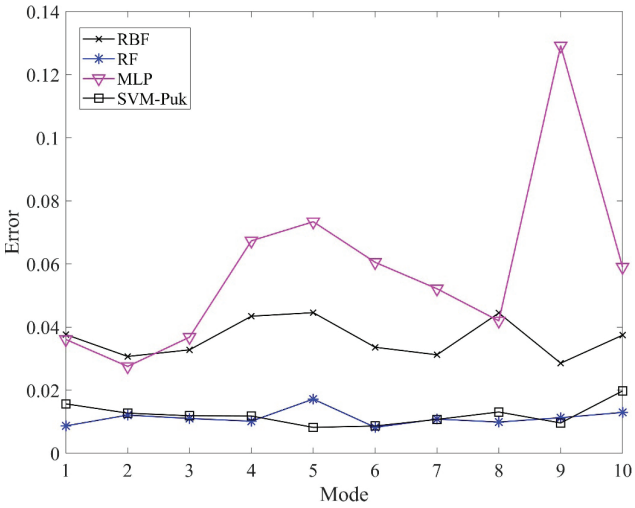

Figure 9. Average prediction error of all machine learning models considering all boundary conditions and length-thickness ratios length-thickness ratios.

CONCLUSIONS

In this study, the prediction of the first ten natural frequencies of very thin, thin, and thick beams has been investigated using RBF Regressor (RBF Reg.), Random Forest Regressor (RF), Multilayer Perceptron Regressor (MLP), and Support Vector Machine Regressor with Puk kernel (SVM-Puk). The prediction analyses have been conducted using a dataset obtained by performing the Finite Element Free Vibration Analysis of beam structures under fixed-free, fixed-simply supported, and simply supported boundary conditions, considering Euler-Bernoulli and Timoshenko Beam Theories. The prediction analysis results have been measured by considering the statistical metrics and prediction performance of the machine learning models considering structural thickness, boundary conditions, and natural frequencies. Therefore, the following conclusions have been drawn.

- All machine learning models have successfully predicted the first ten natural frequency values of thick structures for all boundary conditions. Therefore, RBF Reg, RF, MLP, and SVM-Puk are powerful machine learning models for predicting the natural frequencies of thick beam structures.
- SVM-Puk and RF models have predicted the first ten natural frequencies of very thin, thin, and thick beams, accurately. The structural thickness-based average accuracy values of the SVM-Puk model are 99.29% for B1, 99.55% for B2, and 97.5% for B3, while they are 99.17%, 98.84%, and 98.71% for RF, respectively. On the other hand, the prediction performance of RBF Reg. and MLP has been decreased as the thickness of the structure has decreased. The structural thickness-based average prediction

accuracy values of the RBF Reg. model are 98.66% for B1, 97.34% for B2, and 93.17% for B3, while they are 98.12%, 92.34%, and 91.65% for MLP, respectively. It can be concluded that SVM-Puk and RF models are robust to the thickness difference since the average error rates differ in a small range. The errors change between 0.45% and 2.5% for SVM-Puk and 0.93% and 1.29% for RF. On the other hand, RBF Reg. and MLP models are sensitive to different thickness values of the beam structures due to the high range of their average error rates. The error rates fluctuate between 1.34% and 6.93% for RBF Reg., while they change between 1.78% and 8.35% for MLP.

- The prediction performance of SVM-Puk and RF models has not been affected considerably by different boundary conditions. They have predicted the first ten natural frequency values accurately, regardless of boundary conditions. Considering the boundary condition-based accuracy values, the SVM-Puk model predicted the first ten natural frequencies by 99.36% for FF, 99.70% for FSS, and 97.80% for SS, while they are 99.19%, 99.01%, and 98.81% for RF, respectively. On the other hand, the prediction performance of RBF Reg. and MLP has been considerably affected as the boundary conditions have changed. The boundary condition-based accuracy values of RBF Reg. are 98.47% for FF, 97.02% for FSS, and 92.28% for SS. For the MLP model, these values are evaluated as 98.38%, 91.25%, and 90.43% respectively. Therefore, RBF Reg. and MLP models are much more sensitive than SVM-Puk and RF to different boundary conditions of the beam structures.
- The prediction results indicate that RF and SVM-Puk are the most effective models for predicting the first ten natural frequency values of the very thin, thin, and thick beams under various boundary conditions. The prediction errors of these models vary between 1% - 2% per frequency, while the average errors have been evaluated as 1.22% and 1.12%, respectively. Therefore, the overall prediction accuracy is 98.88% For RF and 98.78% for SVM-Puk. Those values become 96.36% and 94.17% for RBF Reg. and MLP, respectively.
- It is seen that MLP model can predict the fundamental frequency of the very thin structures by an average accuracy of 99.34%. For thin and thick structures RF shows the best performance by an average accuracy of 99.48%.
- The prediction analysis results of this study indicate that the SVM-Puk can be a powerful alternative regression machine learning model for various structural engineering problems.
- The prediction performance of the RBF Reg model is good for the thick beams and thin beams. However, the prediction accuracy considerably has decreased for very thin beams. Therefore, it has been concluded that RBF Reg is an effective model for thick and thin beams while it is not suitable for very thin beams.
- Considering the success of the RF model, it is suggested that the effectiveness of that model should be investigated more deeply for various cases of structural engineering.

AUTHORSHIP CONTRIBUTIONS

Authors equally contributed to this work.

DATA AVAILABILITY STATEMENT

The authors confirm that the data that supports the findings of this study are available within the article. Raw data that support the finding of this study are available from the corresponding author, upon reasonable request.

CONFLICT OF INTEREST

The author declared no potential conflicts of interest with respect to the research, authorship, and/or publication of this article.

ETHICS

There are no ethical issues with the publication of this manuscript.

REFERENCES

[1] Kam M, Saruhan H. Vibration damping capacity of deep cyrogenic treated AISI 4140 steel shaft supported by rolling element bearings. Mater Test 2021;63:742–747. [CrossRef]

[2] Hirane H, Belarbi MO, Houari MSA, Tounsi A. On the layerwise finite element formulation for static and free vibration analysis of functionally graded sandwich plates. Eng Comput 2021;38:3. [CrossRef]

[3] Kam M. Effects of deep cyrogenic treatment on machinability, hardness and microstructure in dry tuning process of tempered steels. P I Mech Eng E-J Pro 2020;235:927–936. [CrossRef]

[4] Do VNV, Lee CH. Static bending and free vibration analysis of multilayered composite cylindrical and spherical panels reinforced with graphene platelets by using isogeometric analysis method. Eng Struct 2020; 215:110682. [CrossRef]

[5] Kam M, Demirtaş M. Experimental analysis of the effect of mechanical properties and microstructure on tool vibration and surface quality in dry tuning of hardened AISI 4340 steels. Surf Rev Lett 2021;28:1–13. [CrossRef]

[6] He JH. Generalized variational principles for buckling analysis of circular cylinders. Acta Mech 2020;231:899–906. [CrossRef]
[7] Kam M, Demirtaş M. Analysis of tool vibration and surface roughness during turning process of tempered steel samples using Taguchi method. P I Mech Eng E-J Pro 2021;235:1429–1438. [CrossRef]
[8] Bagheri B, Abdollahzadeh A, Sharifi F, Abbasi M. The role of vibration and pass number on microstructure and mechanical properties of AZ91/SiC composite layer during friction stir processing. P I Mech ENG C-J Mech Eng Sci 2022;236:2312–2326. [CrossRef]
[9] Kam M, Şeremet M. Experimental and statistical investigation of surface roughness and vibration during finish turning of AISI 4140 steel workpiece under cooling method. Surf Rev Lett 2021;28:10. [CrossRef]
[10] Şengül Ö, Kam M. Analysis of radial tire design and dynamic analysis for sustainable production. IMASCON 2019; Kocaeli, Turkey.
[11] Daş DB, Birant D. Ordered physical human activity recognition based on ordinal classification.Turk J Electr Comput Sci 2021;29:2416–2436. [CrossRef]
[12] Zhan Z, Li H. A novel approach based on the elastoplastic fatigue damage and machine learning models for life prediction of aerospace alloy parts fabricated by additive manufacturing. Int J Fatigue 2021;145:106089. [CrossRef]
[13] Kardani N, Zhou A, Nazem M, Shen SL. Estimation of Bearing Capacity of Piles in Cohesionless Soil Using Optimised Machine Learning Approaches. Geotech Geol Eng 2020;38:2271–2291. [CrossRef]
[14] Boiangiu M, Ceausu V, Untaroiu CD. A transfer matrix method for free vibration analysis of euler-bernoulli beams with variable cross section. J Vib Cont 2016;22:2591–2602. [CrossRef]
[15] Chen M, Jin G, Zhang, Y, Niu F, Liu Z. Three-dimensional vibration analysis of beams with axial functionally graded materials and variable thickness. Comp Struct 2019;207:304–322. [CrossRef]
[16] Pradhan KK, Chakraverty S. Natural frequencies of shear deformed functionally graded beams using inverse trigonometric functions. J Braz Soc Mech Sci 2017;39:3295–3313. [CrossRef]
[17] Hong CC. Free vibration frequency of thick FGM spherical shells with simply homogeneous equation by using TSDT. J Braz Soc Mech Sci 2020;42:159. [CrossRef]
[18] Laory I, Trinh TN, Smith IFC, Brownjohn JMW. Methodologies for predicting natural frequency variation of a suspension bridge. Eng Struct 2014;80:211–221. [CrossRef]
[19] Avcar M, Saplioglu K. An artificial neural network application for estimation of natural frequencies of beams. Int J Adv Comput Sci Appl 2015;6:94–102. [CrossRef]
[20] Dey S, Mukhopadhyay T, Spickenheuer A, Gohs U, Adhikari S. Uncertainty quantification in natural frequency of composite plates - an artificial neural network based approach. Adv Comp Lett 2016;25:43–48. [CrossRef]
[21] Banerjee A, Pohit G, Panigrahi B. Vibration analysis and prediction natural frequencies of cracked timoshenko beam by two optimization techniques - cascade ann and anfis. Mater Today Proceed 2017;4:9909–9913. [CrossRef]
[22] Nikoo M, Hadzima-Nyarko M, Nyarko EK, Nikoo M. Determining the natural frequency of cantilever beams using ann and heuristic search. Appl Artif Intelligence 2018;32:309–334. [CrossRef]
[23] Karsh PK, Mukhopadhyay T, Dey S. Stochastic investigation of natural frequency for functionally graded plates. IOP Conf Ser Mater Sci Eng 2018;326:012003. [CrossRef]
[24] Ali F, Chowdary BV. Natural frequency prediction of fdm manufactured parts using ann approach. IFAC-PapersOnLine 2019;52:403–408. [CrossRef]
[25] Atilla D, Sencan C, Goren Kiral B, Kiral Z. Free vibration and buckling analyses of laminated composite plates with cutout. Arch Appl Mech 2020;11:2433–2448. [CrossRef]
[26] Jayasundara N, Thambiratnam DP, Chan THT, Nguyen A. Damage detection and quantification in deck type arch bridges using vibration based methods and artificial neural networks 2020;109:104265. [CrossRef]
[27] Saeed RA, Galybin AN, Popov V. Crack identification in curvilinear beams by using ann and anfis based on natural frequencies and frequency response funcitons. Neural Comput Appl 2012;21:1629–1645. [CrossRef]
[28] Hakim SJS, Razak HA. Structural damage detection of steel bridge girder using artificial neural networks and finite element models. Steel Comp Struct 2013;14:367–377. [CrossRef]
[29] Yan B, Cui Y, Zhang L, Zhang C, Yang Y, Bao Z, Ning G. Beam structure damage identification based on bp neural network and support vector machine. Math Prob Eng 2014;2014:850141. [CrossRef]
[30] De Fenza A, Sorrentino A, Vitello P. Application of artificial neural networks and probability ellipse methods for damage detection using lamb waves. Comp Struct 2015;133:390–403. [CrossRef]
[31] Satpal SB, Guha A, Banerjee S. Damage identification in aluminum beams using support vector machine: numerical and experimental studies. Struct Cont Health Monitor 2015;23:446–457. [CrossRef]
[32] Ghiasi R, Torkzadeh P, Noori M. A machine-learning approach for structural damage detection using least square support vector machine based on a new combinational kernel function. Struct Health Monitor 2016;15:302–316. [CrossRef]

[33] Neves AC, Gonzalez I, Leander J, Karoumi R. Structural health monitoring of bridges: a model-free ann-based approach to damage detection. J Civil Struct Health Monitor 2017;7:689–702. [CrossRef]

[34] Kourehli SS. Prediction of unmeasured mode shapes and structural damage detection using least squares support vector machine. Struct Monitor Maint 2018;5:379–390.

[35] Hassan AKF, Mohammed LS, Abdulsamad HJ. Experimental and artificial neural network ann investigation of bending fatigue behavior of glass fiber/polyester composite shafts. J Braz Soc Mech Sci Eng 2018;40:201. [CrossRef]

[36] Ghiasi R, Ghasemi MR, Noori M. Comparative studies of metamodeling and ai-based techniques in damage detection of structures. Adv Eng Soft 2018;125:101–112. [CrossRef]

[37] Tan ZX, Thambiratnam DP, Chan THT, Gordan M, Razak HA. Damage detection in steel-concrete composite bridge using vibration characteristics and artificial neural network. Struct Infra Eng 2020;16:1247–1261. [CrossRef]

[38] Tran-Ngoc H, Khatir S, De Roeck G, Bui-Tien T, Wahab MA. An efficient artificial neural network for damage detection in bridges and beam-like structures by improving training parameters using cuckoo search algorithm. Eng Struct 2019;199:109637. [CrossRef]

[39] He M, Wang Y, Ramakrishnan KR, Zhang Z. A comparison of machine learning algorithms for assessment of delamination in fiber-reinforced polymer composite beams. Struct Health Monitor 2020;20:1997–2012. [CrossRef]

[40] Gan BS. An isogenometric approach to beam structures. Cham, Springer; 2018. [CrossRef]

[41] Frank E. Fully supervised training of gaussian radial basis function networks in WEKA. 2014.

[42] Breiman L. Random forests. Mach Learn 2001;45:5–32. [CrossRef]

[43] Hastie T, Tibshirani R, Friedman J. The elements of statistical learning. New York, Springer-Verlag, NY:Springer; 2009. [CrossRef]

[44] Stathakis D. How many hidden layers and nodes?. Int J Remote Sens 2007;30:2133–2147. [CrossRef]

[45] Uzair M, Jamil N. Effects of hidden layers on the efficiency of neural networks. 2020 IEEE 23rd Int Multitopic Conf. [CrossRef]

[46] Tran TTK, Lee T, Kim JS. Increasing neurons or deepening layers in forecasting maximum temperature time series?. Atmoshpere 2020;11:1072. [CrossRef]

[47] Smola AJ, Schölkopf B. A tutorial on support vector regression. Stat Comput 2004;14:199–222. [CrossRef]

[48] Üstün B, Melssen WJ, Buydens LMC. Facilitating the application of support vector regression by using a universal pearson vii function based kernel. Chemometr Intell Lab Syst 2006;81:29–40. [CrossRef]